Lightweight Whiskers for Contact, Pre-Contact, and Fluid Velocity Sensing

William Deer and Pauline E. I. Pounds

***Abstract*—This letter reports the design, fabrication, and testing of lightweight whisker sensors intended for use on robotic platforms, especially drones, featuring multiple whisker fibers in an array. The whiskers transmit forces along the vibrissae fibers to a load plate bonded to embedded MEMS barometers potted in polyurethane rubber, which act as force sensors. This construction allows for directional sensing of forces with arrays of fibers weighing less than half a gram per whisker. Forces as low as 3.33 μN can be measured, and the whiskers are capable of sensing fluid stream velocities up to 7.5 m·s^{-1}. The whiskers are sufficiently sensitive so as to be able to detect the pressure wave of an approaching hand moving at 0.53 m·s^{-1} from 20 mm away.**

***Index Terms*—Robot sensing systems, tactile sensors, fluid flow measurement.**

I. Introduction

CONTACT and proximity sensing are important capabilities for robots interacting with the world, and in particular humans. The ability to anticipate contact and take appropriate action is especially needed when operating in close proximity to people. Thus, a sensor modality that can detect contact and pre-contact forces — where preceding air pressure from an approaching object is sensed prior to contact — is very useful. A natural example of such devices are whiskers, or "vibrissae", commonly found on animals as diverse as rats, cats, dogs, horses and seals. These devices provide animals with useful information about obstacles, near-by movement in the form of vibrations and air pressure, and speed through the water [1].

In particular, we are interested in translating the proven sensor utility of whiskers on ground platforms to hovering robots and drones — whiskers that can sense low-force contact with the environment such that the robot can manoeuver to avoid more dangerous, high-force interactions. We are motivated by the task of navigating through dark, dusty, smoky, cramped spaces, or gusty, turbulent environments with micro-scale aircraft that cannot mount heavier sensors such as lidars. This requires the development of robust, light weight, sensitive, compact sensors in an economical form. Researchers have begun exploring the possibility of integrating contact probes and whiskers with drones, such as the EPFL Euler spring contact VTOL [2] and [3] but the full potential for such devices has yet to be explored.

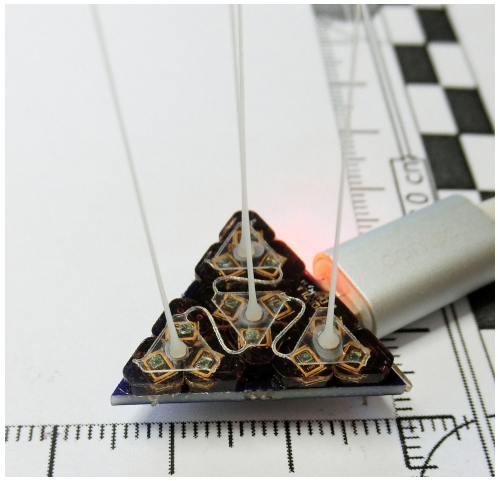

Fig. 1. Miniature Embedded Whisker Sensor on PCB.

Previous work to produce whiskers for terrestrial robotics has had a strong focus on the perceptive function of whiskers — for example, using active devices to model the environment [4] or sense object geometry [5]. The sensing modalities explored have exploited physics such as electret microphone diaphragms [6], hall effect sensors [7], and strain gauges in addition to many others [4]. A substantial fraction of this work has focussed on the frequency response characteristics of the whiskers, with the expectation of their application to texture sensing [6]. We perceive a gap in the current body of work in which very low-cost, light-weight whiskers may measure both contact and fluid motion (specifically air and water) — moving away from structural perception to instead provide lower-level navigation input for hovering vehicles.

Our approach is to build upon the authors' previous work in developing rotor force sensors for quadrotors by placing a semi-rigid fibre on a load plate atop a multi-element load cell [8]. The load cells comprise MEMS barometers embedded in polyurethane rubber, and provide sub-gram sensitivity [9]. By incorporating light-weight extruded fibres onto a tessellated array of miniaturized versions of the load cell, a dense sensing fur

Manuscript received September 10, 2018; accepted January 19, 2019. Date of publication February 13, 2019; date of current version February 28, 2019. This letter was recommended for publication by Associate Editor A. Elfes and Editor J. Roberts upon evaluation of the reviewers' comments. This work was supported by the Asian Office of Aerospace Research and Development/Air Force Office of Scientific Research under Grant FA2386-16-1-4026. *(Corresponding author: Pauline E. I. Pounds.)*

The authors are with the School of Information Technology and Electrical Engineering, The University of Queensland, Brisbane, QLD 4072, Australia (e-mail: w.deer@uq.edu.au; pauline.pounds@uq.edu.au).

This letter has supplementary downloadable material available at http://ieeexplore.ieee.org, provided by the authors. The Supplementary Materials contain a video showing the light-weight whiskers for contact, pre-contact and fluid velocity sensing as described in the paper. This material is 5.02 MB in size.

Digital Object Identifier 10.1109/LRA.2019.2899215

TABLE I
WHISKER DESIGN REQUIREMENTS

Weight	<5 g	Array size	4–10 fibres
PCB Size	10–30 mm	Sensitivity	<1 g
Whisker length	10–100 mm	Resolution	>100 Hz
Interface	USB, UART	Reaction time	<10 ms

may be constructed (see Fig. 1). There are numerous approaches, with associated tradeoffs, to be explored.

In this letter, we present a compact, embedded whisker sensor design. Section II describes the construction of the whiskers, including the sensing element and whisker fibre fabrication. Section III reports experiments to characterise the sensor performance in contact sensing, pre-contact sensing and fluid velocity sensing. Section IV contains a discussion on the performance and practical application of the devices. A brief conclusion completes the letter.

II. CONSTRUCTION

The whisker devices are intended to be static vibrissae sensors[1] (ie. no whisking actuation), with the primary intention that they can be deployed on 200 g quadrotor platforms for experiments with obstacle avoidance and velocity control, with additional application to platforms such as water velocity sensing for surface craft, robot rats [10] for rat neuroscience/cognitive science studies and humanoid robots such as the University of Queensland's 'Opie' partial humanoid for child interaction [11]. These applications motivate the design requirements set out in Table I.

The design paradigm is to construct arrays of hairs on tesselateable printed circuit board tiles. Each whisker element consists of the PCB and processor, sensing element force pads, a load distributing plate, and the fibre itself. The flexible whisker is bonded to the load plate, which transmits forces to a trio of sensing force pads — in this way, direction and magnitude of contact force at the tip of the fibre may be inferred. The method of actuation is similar in principle to Charalambides and Bergbreiter's elastic MEMS concept [12], except in this case the fibre is adhered to a load plate with vertically oriented discrete sensors, whereas their 2016 work uses a vertical pillar with laterally oriented sensors in an integrated unit. The simpler construction of discrete COTS MEMS devices offers potentially lower-cost fabrication.

Fabrication onto a PCB allows the sensing element and communication system to be tightly integrated, and each follicle module can be compact enough to be incorporated into artificial skin, either directly or attached to a flex-PCB bus.

Localised intelligence at each fibre allows for low-level signals of interest to be discriminated and prioritised over bulk reads so that contacts and fluid velocity step changes can be promptly detected and responded to. This is noted to be especially important in social robotics, where instantaneous responses to physical cues are considered key to life-like agency [13]. The processor used is an STM32F042, with a simple sensor magnitude threshold used to determining events of interest; an off-board script applies a 101-sample window Sovitsky-Golay filter. USB communication was selected for its high data rate and support for up to 127 devices. The all-up weight of the four-whisker sensor array is 1.6 g, and the total cost is $20.

[1]The whiskers are suitable for adaptation for an active whisking system, but these are not explored here to avoid inertial coupling. The utility of inertial coupling of these sensors will be considered in future work.

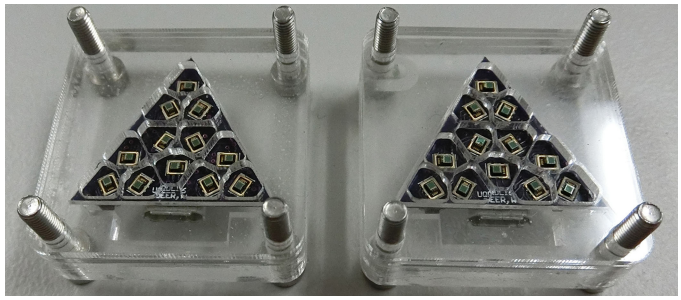

Fig. 2. Uncapped sensors in casting scaffold.

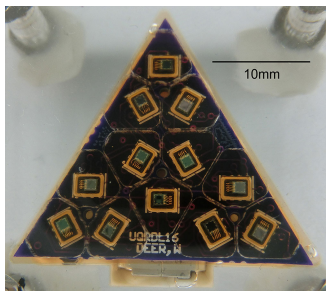

Fig. 3. Embedded force pads in a triangular array.

We discuss each sub component of the whisker and its fabrication below.

A. Force Pads

The force pads leverage the embedded MEMS barometers technique pioneered at Harvard and Takktile Robotics [14], and previously used by the authors for quadrotor rotor force sensing [9], [15]. The sensors used here are Bosch BMP280 barometers, which communicate via I2C and have a temporal resolution of 157 Hz. The metal cans containing the MEMS devices are removed to directly expose the sensing elements and an laser-cut acrylic stencil is used to form a potting mould around each sensor (see Fig. 2). Vytaflex Shore 20 polyurethane is degassed with an Easy Composites degassing chamber at 99 per cent vacuum, then cast around the devices. Once set, the stencil is removed, leaving each pad an independent unit. The pads are fabricated en masse, arranged in triangular sets of three per fibre (see Fig. 3).

B. Load Plate

The load plates transfer whisker tip force into force triples at the base of each fibre. The fabrication process for these components must be low-cost, easily scalable and low-complexity in manufacture. As the fibre and sensor units decrease in size, the difficulty in assembling the devices will increase; the process must be feasible for arrays of hundreds of units. Thus, a batch

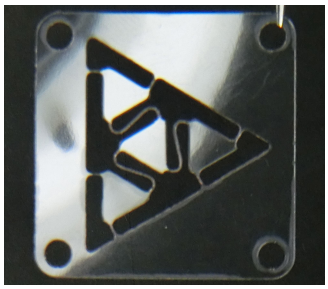

Fig. 4. Laser-cut load plates with connecting flexible "S" links.

laser cut technique was used, in which multiple load plates are cut from a single sheet of material simultaneously (see Fig. 4).

Greenfield 0.13 mm sheet polystyrene was chosen for the load plates as it is available in thin sheets and is light weight, but has good dimensional tolerance and adheres well to cured Vytaflex with gel cyanoacrylate. It also has the property of being thermoplastic in a similar range to ABS — used for the whisker fibres — melting at 240 °C, which is equal to the extrusion temperature of most ABS printer heads.

Each load plate is connected to its neighbors by flexible "S" links. These inter-links maintain the spatial position of each plate relative to its neighbors and to alignment posts used for assembling the whisker array. Once cut and loaded with fibres, the set of plates is bonded to the force pads, allowed to cure, and then the alignment post scaffold is cut free. The flexible geometry of the "S" links means that they do not need to be cut during operation, eliminating an otherwise labour intensive post-process.

C. Fibre Fabrication

Two methods were explored for fibre fabrication: extrusion from ABS onto polystyrene sheet and 3D printing with flexible polymer, along with a hybrid combination of the two techniques; both offer different benefits for fabrication.

1) Extruded Fibres: Fibre extrusion uses a "taffy pull" approach, in which the vertical motion, temperature and feed rate of a filament 3D printer is used to modulate the thickness and elongation of plastic threads drawn from a deposited blob of hot plastic. This allows differing lengths and tapers of vibrissae to be achieved for different applications — eg. short fibres for high-speed fluid velocity sensing vs long fibres for low-speed sensing. ABS was chosen as the test material due to its demonstrated prior use as vibrissae [7], ready application in stock 3D printers, and easy thermo-adhesion to sheet styrene. This technique allows a forest of fibres to be deposited and extruded on a single sheet quite quickly, with custom distribution and positioning of each fibre.

Several combinations of settings were tested in drawing the fibres, with the goal of producing even fibres of roughly constant 0.4 mm width for arbitrary lengths. An XYZPrinting Da Vinci 1.0 3D printer with custom firmware allowing direct G code execution was used so as to provide complete control over the parameters of the operation.

The fibres were drawn by depositing a starting bead of ABS onto the load plate at 220 °C and holding position while a small amount of additional molten material is added by the feeder. The build platform is maintained at 110 °C. This allows the heat from the blob to locally melt and combine with the load plate to create strong adhesion. After 2.1 seconds, the head is then raised vertically at 2.916 mms^{-1} while material is fed in at 0.146 mms^{-1}. Using a 0.4 mm nozzle, small variations in draw and feed rate allow different geometries from 0.2–0.4 mm in thickness and 3–150 mm in length to be achieved. The length of the fibres was limited only by the vertical dimension of the 3D printer used.

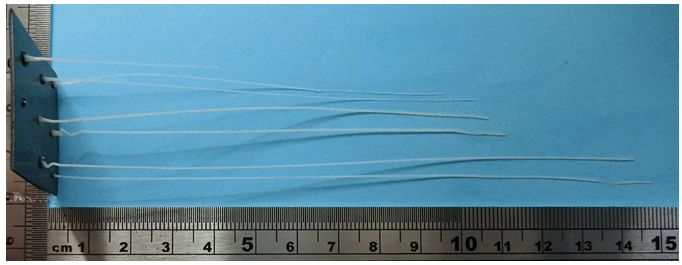

Fig. 5. Extruded whisker fibres fused to polystyrene sheet.

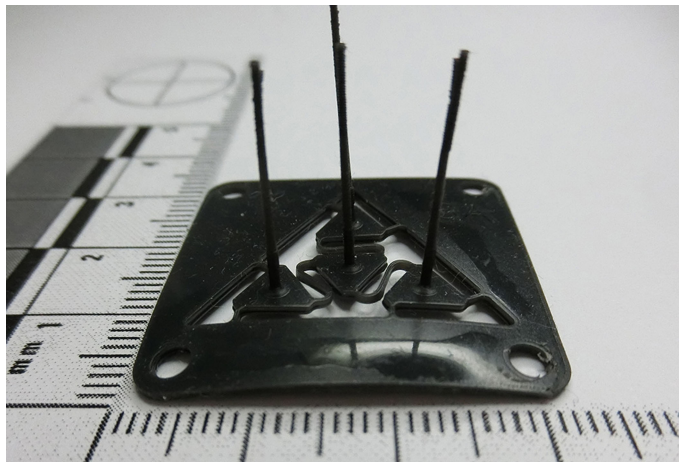

Fig. 6. Printed whisker fibres on integrated load plate.

If the fibres are drawn too quickly, or the feed rate is too slow, they will thin out and separate from the build head. If extruded too quickly or drawn too slowly, the fibres will bunch up and coil — this is especially noticeable when forming the initial blob to bond the fibre to the load plate (see Fig. 5).

2) Printed Fibres: A limitation of ABS extrusions is the permanent fusion of the fibres to the load plate: if a fibre is damaged or breaks, it is lost and cannot easily be restored without replacing the load plate. Thus direct extrusion is relatively costly to maintain for bulk arrays of fibres. An alternative process was explored in which arrays of fibres were directly printed using a flexible SLA resin with a Formlabs Form 2 printer. The load plate and fibres are produced as a single integral piece, such that the entire mechanical component is produced in one automated step (see Fig. 6).

There are two key concerns of this approach: 1. the minimum achievable thickness of the fibres, and 2. the cyclic loading lifetime of fibres fabricated in this way. The first was resolved by printing an array of fibres from 0.1 mm to 1 mm in thickness, at a length of 50 mm. It was found that fibres 0.5 mm thick could

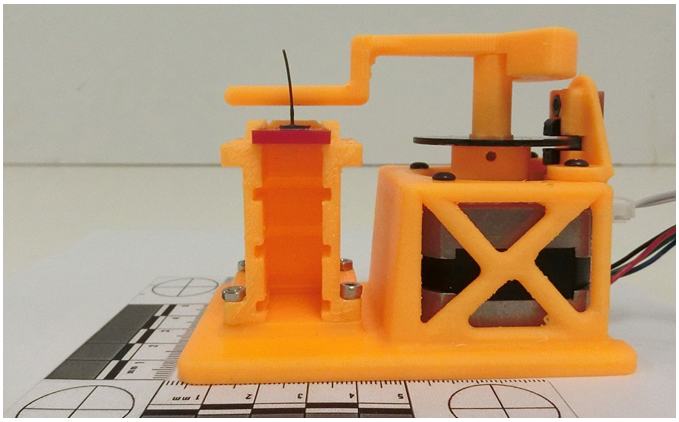

Fig. 7. Cyclic whisker loading test apparatus with whisker tested beyond one million cycles.

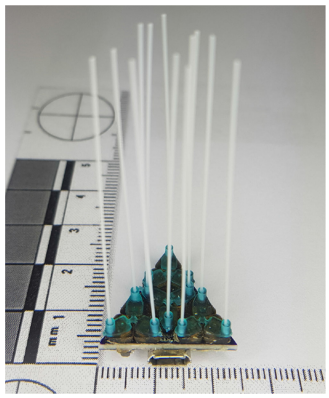

Fig. 8. Hybrid printed-extruded array.

be produced reliably with tapers down to 0.25 mm, but only to a length of 40 mm; thin fibres longer than this would fail. The life-cycle time of these fibres was tested with an automatic loading device consisting of a sweeping arm driven by a NEMA17 (JLB 17HS1352-P4130) stepper motor (see Fig. 7). It was found that test fibres withstood over one million flexure cycles at 1 Hz loading without failing (7×10^6 seconds over 11.57 days), at which point the test was ended.

3) Hybrid Array: To combine ease of production of long, thin fibres with lifetime and repairability, we integrated ABS extruded fibres with a 3D printed base. In this way, arbitrarily long fibres may be used with rapidly 3D printed bases, and when a fibre breaks it can be individually replaced by regluing it. The 3D printed base no longer needs to be flexible — it is modified to have sockets for fibres, which are more reliable to print than fibres. Once the load plate is glued to the force pads, ABS fibres are easily inserted using a jig (see Fig. 8). During first installation, residual UV cure resin can be used as a glue by exposing freshly produced parts to UV light once fibres are installed, but prior to rinsing with alcohol. This technique allows the fibres to be installed at a variety of non-perpendicular angles to the load plate.

D. Thermal Calibration

The MEMS barometers use manufacturer-tuned parameters to compute temperature and a calibrated pressure value [16]. Potted sensors deviate from the thermal profile of free air sensors, due to self-heating inside the rubber encapsulant. A 6.7 ms^{-1} step change in fluid velocity generated by the test rig described in Section III-C applied to a whisker led to a diverging measurement, even when the applied force was held constant after the step (see Fig. 9); an unpotted sensor on the same board did not exhibit this drift. Following the applied transients, a residual error persists — believed to be due to convective cooling. Mechanical hysteresis was excluded as the cause due to the time-varying characteristics of the observed behaviour.

From this we surmise that the constant parameters given by the manufacturer to compensate for thermal dynamics of the sensors do not account for non-air media. Tuning parameters are either common across all BMP280 devices, or uniquely matched to individual devices; given a known input force, the appropriate parameters may be manually constructed by adjusting the common parameters. It was found that for 2 mm thick Vytaflex, appropriate custom values are $D_{T1} = 27140$, $D_{T2} = 25987$, $D_{P1} = 37569$, $D_{P2} = -10764$, $D_{P4} = 859$, $D_{P5} = 197$, $D_{P6} = 2000$.

III. Experiments

The sensors were verified for basic operation and then tested for performance. Each whisker of the sensor array is capable of detecting both magnitude and direction of applied force at its tip — the individual sensor values are summed along 120° basis directions to produce a vector force magnitude and direction that is returned to the host. When the array is swept over a textured or smooth surface, the resulting force map may be streamed in real time to a visualisation front-end, mapped as the sum of scaled magnitude of 120° basis vectors corresponding to each sensor, as shown in the video attachment and Fig. 10. Three sets of experiments were used to test the three uses of the sensors: contact, pre-contact and velocity measurement. In each experiment, the sensor is oriented such that the predominant axis of applied forces runs parallel to the edge of the circuit board — the least sensitive configuration — where no single sensor is in alignment with the transmitted force moment. The performance testing reported in this letter was conducted with 50 mm extruded ABS fibres bonded to polystyrene sheet. The 3D printed and hybrid construction techniques reported in Section II-C will be tested as part of future work.

A. Contact Force Sensing

Contact force measurement was evaluated by applying force to the whisker using a contact point attached to a Diamond Professional-Mini precision scale with 196.1 mN range and 0.01 mN resolution. The whisker is mounted on a Panavise lead screw, so that increasing force may be applied by moving the sensor downward against the contact point (see Fig. 11). Force was applied in quarter-turn increments of the leadscrew (approximately 0.49 mm per step), with the resultant scale force and whisker sensor reading recorded; the experiment was repeated

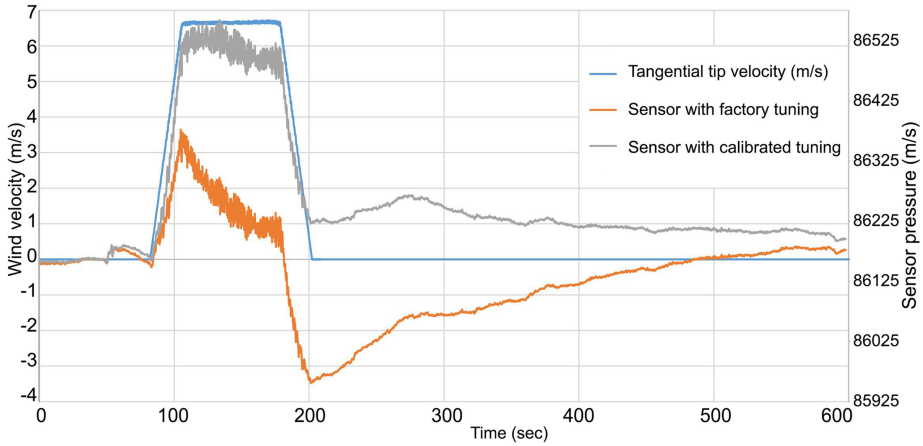

Fig. 9. Compensated and uncompensated sensor measurements with velocity reference.

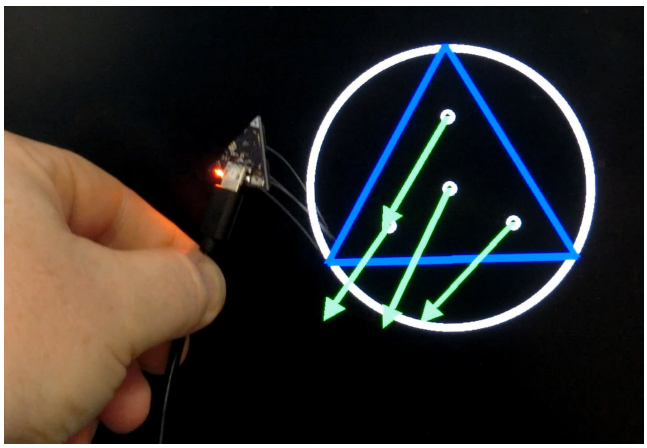

Fig. 10. Visualisation software for whisker tip contact force.

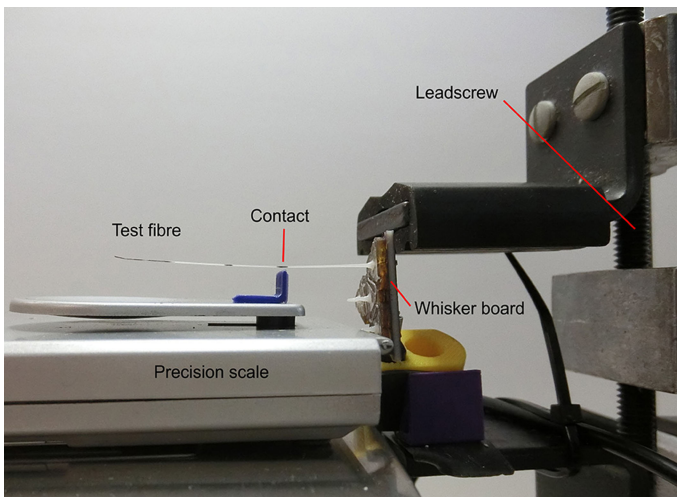

Fig. 11. Incremental contact force linearity test apparatus.

at three points along the whisker: 10 mm, 20 mm and 30 mm from the tip of the whisker (see Fig. 12).

The whiskers are able to measure forces as low as 3.33 μN at 10 mm from the tip and as high as 7.728 mN at 30 mm from

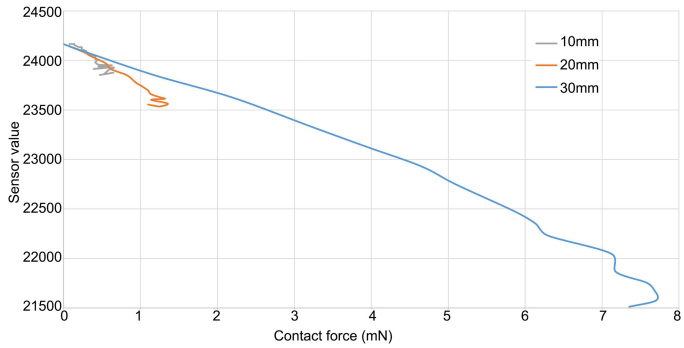

Fig. 12. Contact force linearity.

the tip. The force data is approximately linear with respect to the applied load, up until the whisker deflects to the point of sliding past the contact — at that point, the contact force begins to decrease as the fibre loses contact with the vertical surface of the contact point and transitions to applying a lateral force. The sensitivity to very low forces was highlighted by the whisker's ability to sense the author's breath at 0.5 m away, requiring precautions to avoid influencing measurements.

B. Pre-Contact Sensing

Detecting the "bow-wave" of air pushed ahead of an approaching object requires a long whisker and sensitive pressure transducer. To verify that our system is capable of detecting such events at a useful interval, the sensor was fixed in place with an onboard status LED configured to turn on when a threshold value of whisker force was exceeded on any of its force pads. A high-speed 1000 Fps Casio EX-ZR50 camera with a 100 mm wide image frame recorded the whisker light as a piece of 150 $\times$ 100 mm corflute was moved from out of frame (Fig. 13(a)), towards the whisker (Fig. 13(b)) and then back out of frame (Fig. 13(f)). The experiment was also conducted using a human hand, photographed at 480 Fps. This allowed the time between detection (Fig. 13(c)) and contact with the whisker (Fig. 13(d)), hand velocity and distance from contact to be measured (see Fig. 13). The corflute was moved towards

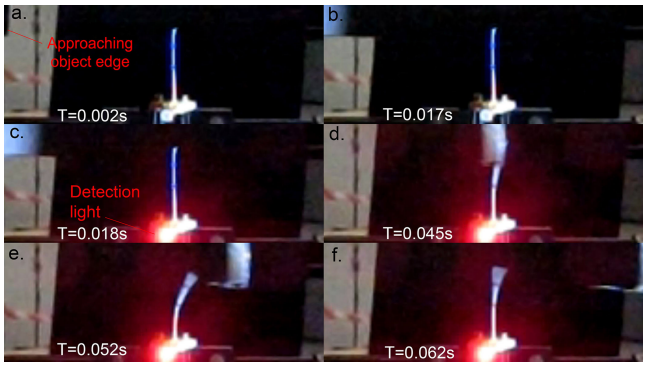

Fig. 13. Pre-contact sensing montage: a. hand entering frame, b. hand approaching, c. hand air pressure detected, d. hand reaches whisker, e. hand clears whisker, f. hand exits frame.

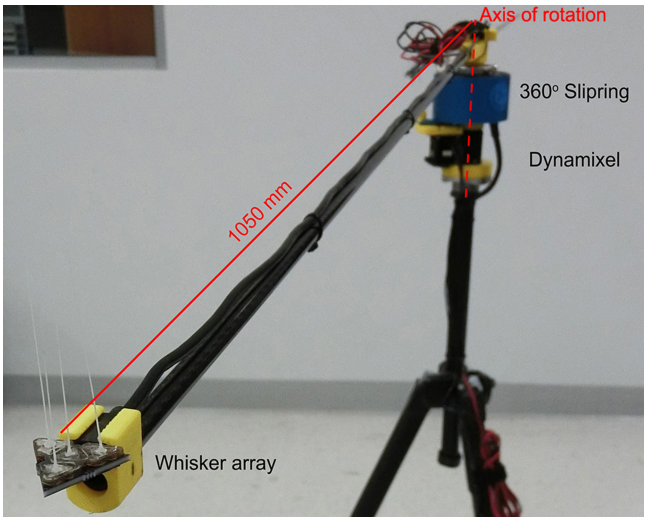

Fig. 14. Whisker fluid velocity sensing swing-arm apparatus.

the whisker at 2.0 ms^{-1}, with the bottom edge 10 mm below the top of the whisker; the approaching edge was detected 40.4 mm from the whisker, 0.044 s before contact. The human hand took 90 frames to pass through the frame (for 0.53 ms^{-1} velocity); the hand was detected 20 mm from the whisker, with 0.037 s warning. Anecdotally, high-speed motions appear easier to detect than low-speed motions. Although 0.04 s provides little warning, it is nevertheless sufficient time for a robot to deenergise its motive systems [17] and thus may prove to be a useful capability.

C. Fluid Velocity Sensing

Fluid velocity sensing was validated using the same sensing apparatus previously used to validate the authors' rotor force sensors [9] — a swing arm revolves at a set velocity, with the test piece at the tip. The apparatus consists of a 1050 mm long tube section driven by a MX-64 Dynamixel motor driven by a USB2Dynamixel interface module with a SNH 025-0410-02S SenRing slip-ring (see Fig. 14); a counterweight set an equal distance away opposite the sensor maintains rotational balance. The Dynamixel is commanded to gradually accelerate and the computed instantaneous tangential velocity of the swing arm tip is compared against the measured sensor value from the whisker (see Fig. 15).

The data show an unexpected ripple superimposed on the measurements. The ripple does not decay over the 24 second-long experiment, suggesting that the effect is not a transient phenomena. All ambient sources of wind disturbance, such as fans and air conditioning, were confirmed to be off. This ripple is in-phase with the rotational orientation of the swing arm, as seen on Fig. 15 by the annotations marking the times where the swing arm passes π rads azimuth. It is believed that the ripple indicates a misaligned tilt of the testing apparatus, such that the fibres' weight applies a sinusoidal bias force.

IV. Discussion

The performance of the whisker sensors meets or exceeds the design goals outlined in Section II. The fabrication technique allows for very dense arrays, and further scope exists to reduce the per-whisker area; the fibre units were expectedly light-weight, with each complete unit weighing 0.4 g per fibre. The linearity of the contact force was very good, especially in the region prior to the contact point sliding. Likewise, the velocity estimate was quite linear with respect to ground truth, but further testing must be carried out to ensure that observed oscillations are artifacts of the apparatus. Otherwise, the excellent sensitivity to contact as well as fluid motion means that they will be adequate for the aerial robotics applications of touch-sensing and velocity sensing for micro robots.

A. Robustness

The sensors with extruded ABS fibres have already been employed on a rat-like robot, the iRat, used to assess its utility in experiments seeking to understand rat behaviour [10].[2] It was found that interactions with biological rats often led to damage to the ABS from the rats chewing on them, leading to several fibres breaking off, which motivated the development of the hybrid 3D printed version which are repairable. Otherwise, the fibres appeared robust during operation. The service life of the sensors has not yet been exceeded in testing.

B. Future Work

The testing reported in this letter verifies the functionality of the sensors — future work will explore and expand their utility. Foremost, future testing will see the sensors installed on hovering platforms to show that they are capable of providing useful information in flight. The cyclic behaviour during fluid velocity sensing must be resolved, and potential coupling between vibrations of the aircraft and the oscillatory dynamics of the fibres will be explored. We will aim to fuse the velocity sensing of the whisker array with the onboard flight control to provide a reactive system for gust-rejection.

The development of the hybrid and 3D printed techniques will be continued and samples will be put through the full gamut of tests as performed on the ABS devices. This will indicate

[2]Heath *et al.* did not report on the function of the whiskers, nor their construction, but rather focussed on the exposure of the robot to rats in the testing environment.

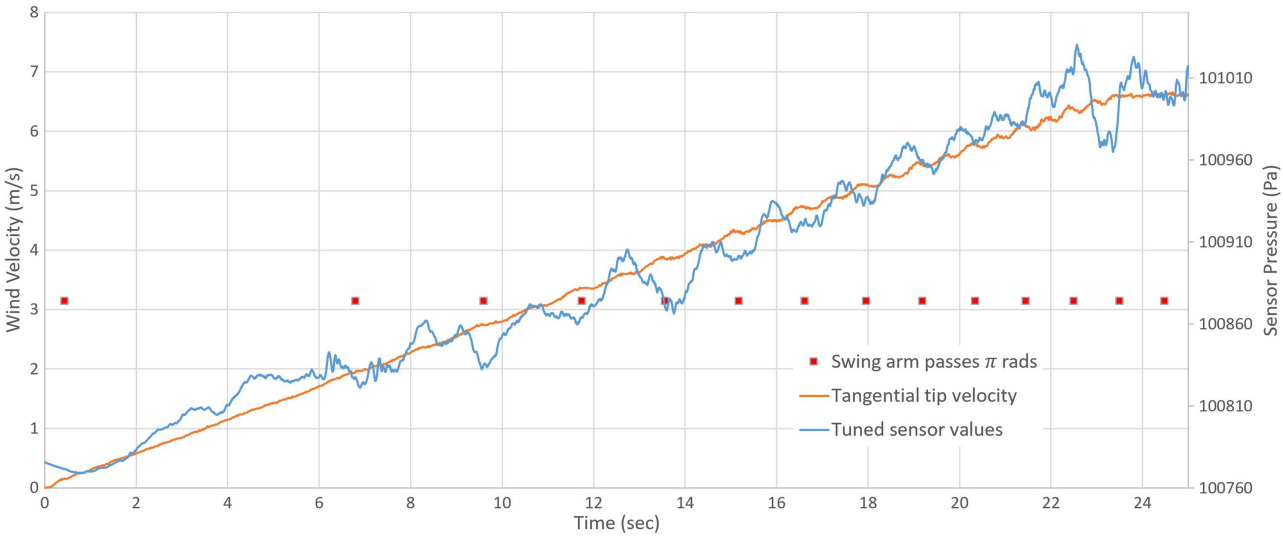

Fig. 15. Whisker fluid velocity linearity.

whether these are suitable alternatives; in particular, the ability to construct whisker arrays with variable vibrissae angles using the hybrid approach will be explored. Denser configurations will also be explored, in which a large array of fibres is locally sub-sampled by pressure transducers in order to extract stronger group signals from fewer expensive devices.

V. Conclusions

This letter reports designs for light-weight, high-sensitivity whiskers for use in robotics, especially aerial robotics applications. The vibrissae are constructed from extruded ABS drawn from a bead of plastic deposited on a polystyrene sheet, mounted on MEMS barometers embedded in Vytaflex, with each directional whisker module weighing 0.4 g. The sensors are able to measure contact forces as low as 3.33 μN, and fluid velocities as high as 7.5 ms^{-1}, with good linearity. The sensors are sufficiently sensitive that impending contacts can be detected from the advancing pressure wave of the approaching object — a hand moving at 0.53 ms^{-1} can be detected with 0.037 s warning at a distance of 20 mm. In addition to the ABS whiskers, we also explored construction techniques including flexible 3D printed SLA material whiskers and hybrid combinations. We believe that this technology will be of use in aircraft-object interaction, collision avoidance and velocity control.

Acknowledgment

The authors would like to thank Jonathon Taufatofua and Prof. Janet Wiles, and the UCSD Chiba Lab for their assistance with this manuscript and iRat testing.

References

[1] W. Hanke *et al.*, "Harbor seal vibrissa morphology suppresses vortex-induced vibrations," *J. Exp. Biol.*, vol. 213, no. 15, pp. 2665–2672, 2010. [Online]. Available: http://jeb.biologists.org/content/213/15/2665

[2] A. Klaptocz, A. Briod, L. Daler, J.-C. Zufferey, and D. Floreano, "Euler spring collision protection for flying robots," in *Proc. IEEE/RSJ Int. Conf. Intell. Robots Syst.*, Nov. 2013, pp. 1886–1892.

[3] S. D. Gollob, Y. Manian, R. S. Pierre, A. S. Chen, and S. Bergbreiter, "A lightweight, compliant, contact-resistance-based airflow sensor for quadcopter ground effect sensing," in *IEEE Int. Conf. Robot. Autom.*, 2018, pp. 7826–7831.

[4] T. J. Prescott, M. J. Pearson, B. Mitchinson, J. C. W. Sullivan, and A. G. Pipe, "Whisking with robots," *IEEE Robot. Autom. Mag.*, vol. 16, no. 3, pp. 42–50, Sep. 2009.

[5] J. A. Wijaya and R. A. Russell, "Object exploration using whisker sensors," in *Proc. Australas. Conf. Robot. Autom.*, 2002.

[6] M. Lungarella, V. V. Hafner, R. Pfeifer, and H. Yokoi, "An artificial whisker sensor for robotics," in *Proc. IEEE/RSJ Int. Conf. Intell. Robots Syst.*, Sep. 2002, vol. 3, pp. 2931–2936.

[7] S. R. Anderson, M. J. Pearson, A. Pipe, T. Prescott, P. Dean, and J. Porrill, "Adaptive cancelation of self-generated sensory signals in a whisking robot," *IEEE Trans. Robot.*, vol. 26, no. 6, pp. 1065–1076, Dec. 2010.

[8] E. Davis and P. E. I. Pounds, "Passive position control of a quadrotor with ground effect interaction," *IEEE Robot. Autom. Lett.*, vol. 1, no. 1, pp. 539–545, Jan. 2016.

[9] E. Davis and P. Pounds, "Direct thrust and velocity measurement for a micro UAV rotor," in *Proc. Australas. Conf. Robot. Autom.*, 2016.

[10] S. Heath *et al.*, "PiRat: An autonomous framework for studying social behaviour in rats and robots," in *Proc. IEEE/RSJ Int. Conf. Intell. Robots Syst.*, 2018, pp. 7601–7608.

[11] S. Heath *et al.*, "Spatiotemporal aspects of engagement during dialogic storytelling child-robot interaction," *Frontiers Robot. AI*, vol. 4, 2017, Art. no. 27. [Online]. Available: https://www.frontiersin.org/article/10.3389/frobt.2017.00027

[12] A. Charalambides and S. Bergbreiter, "Rapid manufacturing of mechanoreceptive skins for slip detection in robotic grasping," *Adv. Mater. Technol.*, vol. 2, no. 1, Art. no. 1600188. [Online]. Available: https://onlinelibrary.wiley.com/doi/abs/10.1002/admt.201600188

[13] G. Durantin, S. Heath, and J. Wiles, "Social moments: A perspective on interaction for social robotics," *Frontiers Robot. AI*, vol. 4, 2017, Art. no. 24. [Online]. Available: https://www.frontiersin.org/article/10.3389/frobt.2017.00024

[14] Y. Tenzer, L. P. Jentoft, and R. D. Howe, "The feel of MEMS barometers: Inexpensive and easily customized tactile array sensors," *IEEE Robot. Autom. Mag.*, vol. 21, no. 3, pp. 89–95, Sep. 2014.

[15] E. Davis and P. E. I. Pounds, "Direct sensing of thrust and velocity for a quadrotor rotor array," *IEEE Robot. Autom. Lett.*, vol. 2, no. 3, pp. 1360–1366, Jul. 2017.

[16] B. Sensortec, "Bmp280 digital pressure sensor," Bosch Sensortec, Tech. Rep., 2018. [Online]. Available: https://ae-bst.resource.bosch.com/media/_tech/media/datasheets/BST-BMP280-DS001-19.pdf

[17] P. E. I. Pounds and W. Deer, "The safety rotor—An electromechanical rotor safety system for drones," *IEEE Robot. Autom. Lett.*, vol. 3, no. 3, pp. 2561–2568, Jul. 2018.